

## Softening behaviour of Fe-6.5%Si steel during warm deformation process

Changsheng Li<sup>a</sup>, Chenglin Yang, Ban Cai, Guojun Cai, and Liqing Chen

State Key Laboratory of Rolling and Automation, Northeastern University, 110819 Shenyang, PR China

**Abstract.** To investigate the softening behaviour during warm deformation process, thermal compression experiment of Fe-6.5%Si silicon steel was conducted. To study the relationship between stress and strain at different strain rate, the investigation of the microstructure, hardness as well as ordered phase constituent of the rolled parts was carried out, respectively. At strain less than or equal to 0.3, micro-hardness was observed to increase with increasing strain. For strain greater than 0.3, the micro-hardness decreased with increasing strain. Indentation morphology of Vickers hardness reveals that the sink-in deformation occurs as the steel has a higher strain-hardening exponent, while pile-up deformation takes place at a lower strain-hardening exponent. Brittle B<sub>2</sub> (FeSi) and DO<sub>3</sub> (Fe<sub>3</sub>Si) ordered phases exist in Fe-6.5%Si steel. With the increasing strain, the diffraction spot strength of B<sub>2</sub> and DO<sub>3</sub> ordered phase is decreased, resulting in the softening behaviour of the Fe-6.5%Si steel during warm deformation process.

### 1. Introduction

Silicon steel is widely used in the manufacture of transformers, engines and other electric devices, is an important magnetic materials applied in telecommunications and military industry [1]. Silicon content has a great influence on the properties of silicon steel, increasing silicon content lead to a lower magnetostriction, a smaller iron loss and a larger permeability. When silicon content reaches 6.5%, the magnetic permeability attains the maximum value, and the magnetostriction approaches zero to confer Fe-6.5%Si steel the excellent magnetic property. Currently, Fe-6.5%Si alloy is the most desirable material to achieve the efficiency, energy saving and portability for electromagnetic equipment [2, 3].

Although Fe-6.5%Si steel has excellent magnetic properties, it is very difficult to be produced by cold rolling due to its brittleness and poor ductility caused by ordered phase in the steel [4, 5].

Generally, warm rolling is utilised to realize the plastic forming of difficult-to-deform metals, the essence of which is to improve the temperature of workpiece and then make it soften in the deformation process. In order to investigate the softening behaviour during warm rolling process, warm deformation behaviour of Fe-6.5%Si steel is studied in this paper. The work hardening exponent, Vickers hardness

---

<sup>a</sup> Corresponding author: [lics@ral.neu.edu.cn](mailto:lics@ral.neu.edu.cn)

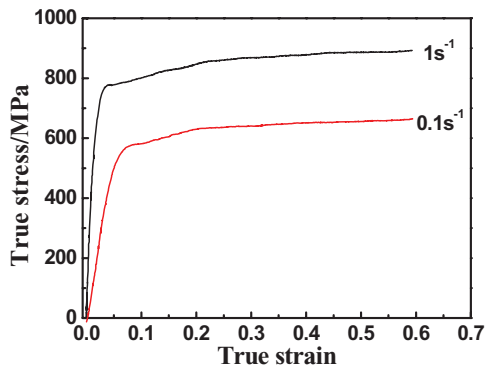


**Figure 1.** Stress-strain curves of Fe-6.5%Si in compression test at 600 °C.

indentation morphology and the ordered phases during warm forming process are analysed. The results will lay the foundation for revealing the warm deformation mechanism of Fe-6.5%Si steel.

## 2. Experimental

Isothermal compression tests were conducted on a MMS-200 thermo-mechanical test frame to investigate the deformation behaviour at 600 °C with strain rate of  $0.1 \text{ s}^{-1}$  and  $1 \text{ s}^{-1}$ , and samples with different true strain (0.1–0.6) were obtained. Samples were immediately quenched after compression. The microstructures of samples after deformation were etched with a 10% solution of nitric acid in alcohol and then observed by a LEICA-DM2500M optical microscopy.

The ordered phases and diffraction patterns were studied using transmission electron microscopy (TEM). The specimens for TEM analysis were made by twin-jet electropolishing in a solution of 5% perchloric acid and 95% ethanol at a voltage of 30V at  $-20 \text{ }^{\circ}\text{C}$ . The thin foils were examined in FEI Tecnai G2 F20 operating at 200 kV. FM-700 micro-hardness indenter was used to measure the Vickers hardness values of the samples at  $50 \mu\text{m/s}$  for 5 s with 500 gf applied load.

## 3. Results and discussion

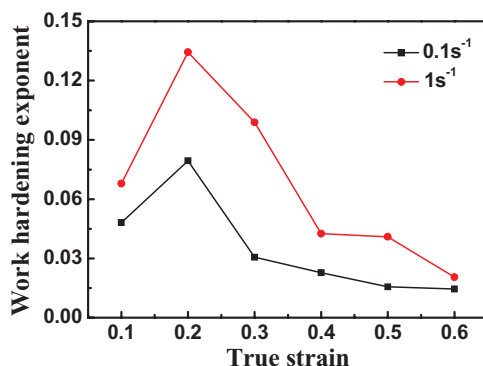
### 3.1 Stress-strain relationship

Figure 1 shows the true stress–strain curve of the Fe-6.5%Si steel under the compression at 600 °C and true strain of 0.6. Flow stress improves remarkably with the increase of strain. The work-hardening effect is very obvious in initial stage of deformation, especially in the region with strain rate of  $1 \text{ s}^{-1}$  where the flow stress rise faster than that of  $0.1 \text{ s}^{-1}$ . With further deformation, the work hardening and dynamic softening reach a dynamic equilibrium, while the dislocation density remains relatively constant and the stress becomes steady state. Since the softening takes place inside the metal, the rate of increase in flow stress is slowed with straining.

Figure 2 shows the relationship between the work-hardening exponent and strain rate. It can be seen that the work-hardening exponent is increasing when the true strain is less than 0.2, and tends to decrease with respect to the true strain exceeding 0.2. This indicates that softening behaviour of the experimental steel has occurred during warm deformation.

### 3.2 Vickers micro-hardness and indentation morphology

Figure 3 shows the relationship between strain and micro-hardness value during compression at 600 °C. It can be seen that when the strain is less than 0.3, the hardness of the sample increases constantly with



**Figure 2.** The work-hardening exponent of Fe-6.5%Si with different strains in compression test at 600 °C.

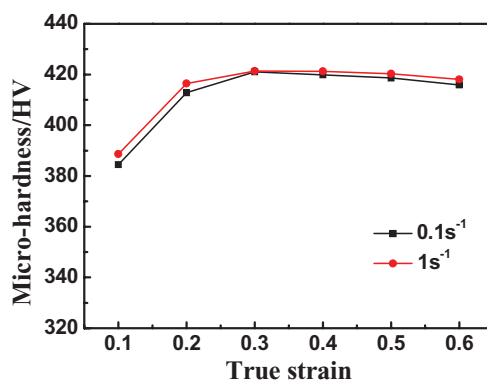


**Figure 3.** The micro-hardness of Fe-6.5%Si at different strain with different strains in compression test at 600 °C.

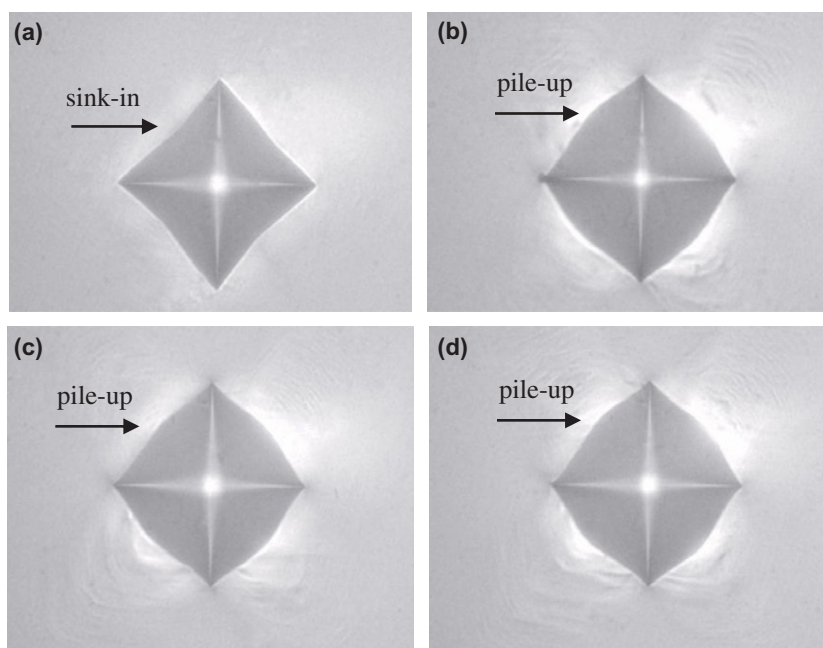
the increase of deformation. It should be attributed to the multiplication of dislocation density which leads to work hardening inside the metal. When the strain is more than 0.3, the hardness value of the sample has a slightly downward trend with the increase of deformation, indicating that the softening effect in the steel is very remarkable.

The micro-indentation morphologies of the samples (600 °C, 1 s<sup>-1</sup>) with respect to different strains are shown in Fig. 4. As can be seen, the surface morphology of undeformed sample exhibits a sink-in deformation mode. Whereas, the deformed samples at true strain of 0.2, 0.4 and 0.6 show higher indentation edges than the initial surface and present a pile-up deformation mode.

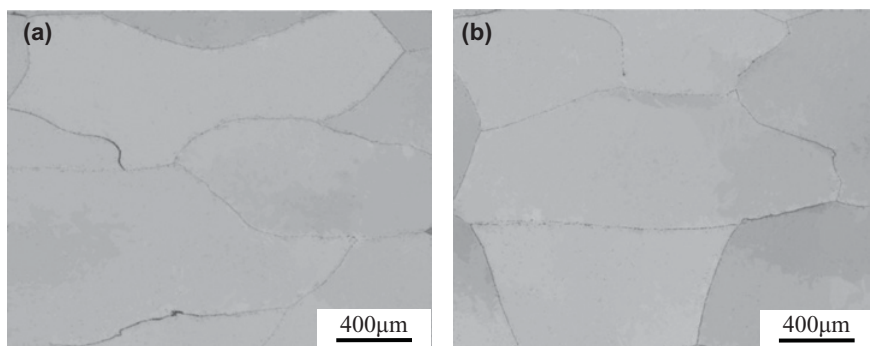
The calculated work hardening exponent of the experimental steel is less than the critical work hardening exponent of 0.259 [6]. With the enhancement of deformation degree, the surface morphology of samples exhibit the pile-up mode and also proves that the experimental steel has generated the softening behaviour.

### 3.3 Microstructure and ordered phases

Figure 5 shows the optical micrograph of Fe-6.5%Si steel after compression ( $\epsilon = 0.3, 0.5$ ) at 600 °C. The grains are elongated perpendicular to the direction of compression and no recrystallisation grain can be found. Therefore, in the process of warm deformation, the strain softening behaviour should be not ascribed to recrystallisation effect [7].



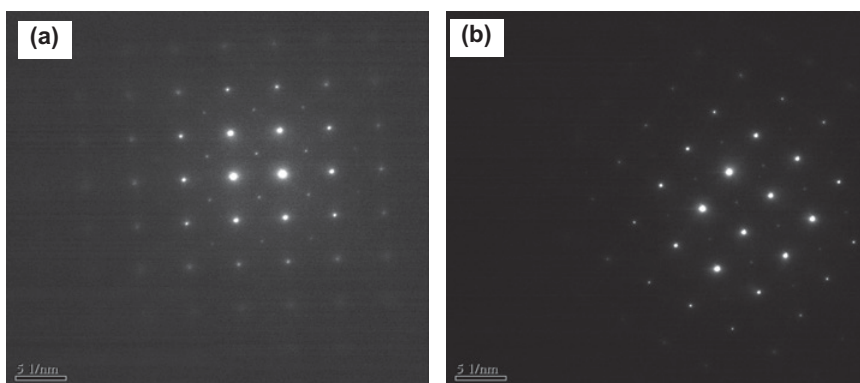
**Figure 4.** Surface morphologies of micro-indentations of samples at different strain. (a)  $\varepsilon = 0$ ; (b)  $\varepsilon = 0.2$ ; (c)  $\varepsilon = 0.4$ ; (d)  $\varepsilon = 0.6$ .



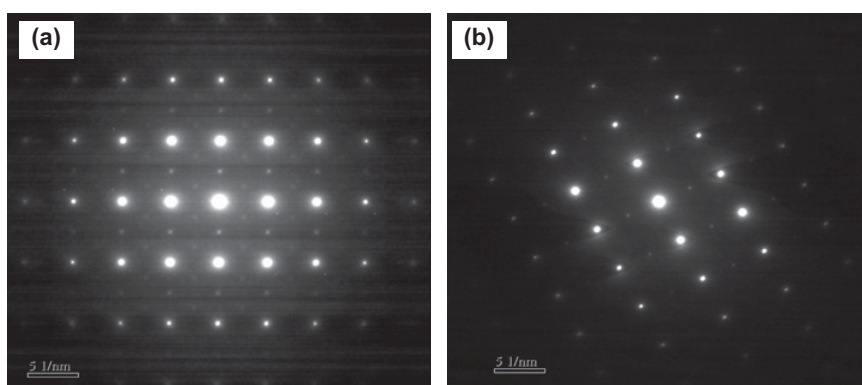
**Figure 5.** The microstructure of samples after warm deformation at strain rate of  $0.1 \text{ s}^{-1}$ . (a)  $\varepsilon = 0.3$ ; (b)  $\varepsilon = 0.5$ .

Figure 6 shows the diffraction patterns of Fe-6.5%Si steel after compression ( $\varepsilon = 0.3, 0.5$ ) at  $600^\circ\text{C}$  along [001] zone axes. The diffraction pattern in Fig. 6 indicates that  $B_2$  (FeSi) ordered phases are formed in the sample at true strain of 0.3. With the strain increasing to 0.6, the  $B_2$  intensity using the (200) superlattice reflection becomes much weaker. Figure 7 shows the diffraction patterns of Fe-6.5%Si steel after compression ( $\varepsilon = 0.3, 0.5$ ) at  $600^\circ\text{C}$  along [011] zone axes. The diffraction pattern in Fig. 6 indicates that  $DO_3$  ( $\text{Fe}_3\text{Si}$ ) ordered phases are produced in the  $\varepsilon = 0.3$  sample. While increasing the strain to 0.6, the  $DO_3$  intensity using the (111) superlattice reflection becomes much weaker.

According to the reciprocal lattice structure factor theory of electron diffraction principle and recent research results [8], the ordered phase diffraction intensity reflects the ordered degree of steel. With the deformation proceeding, the experimental steel generates softening.



**Figure 6.** Diffraction patterns for [001] zone axes of ordered phase of the sample. (a)  $\varepsilon = 0.3$ ; (b)  $\varepsilon = 0.6$ .



**Figure 7.** Diffraction patterns for [011] zone axes of ordered phase of the sample. (a)  $\varepsilon = 0.3$ ; (b)  $\varepsilon = 0.6$ .

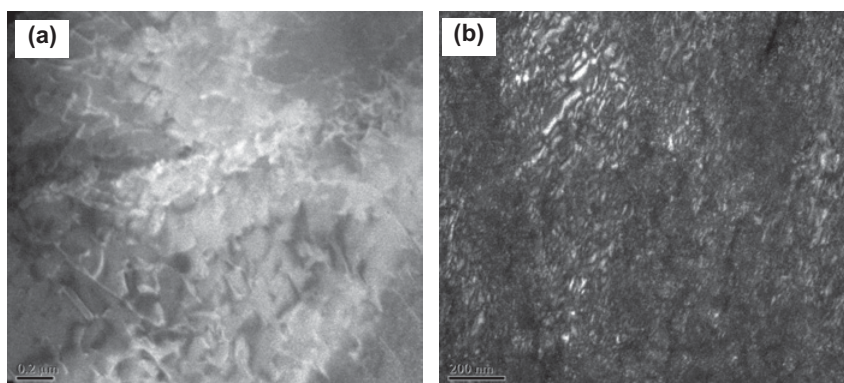


**Figure 8.** TEM dark-field images of deformed samples at different strains. (a)  $\varepsilon = 0.3$ ; (b)  $\varepsilon = 0.6$ .

The dark field image of the ordered phase in the experimental steel with different strain is shown in Fig. 8. Because the different crystal structure of the ordered and disordered phases cause different diffraction conditions, resulting in the different diffraction contrast of the ordered and disordered phases.

According to the TEM diffraction contrast imaging principle, matrix is black contrast in dark field image, while the ordered phases possess white contrast, so it is easy to distinguish the ordered and disordered phases in dark field image.

From above figures, we can clearly see that the white contrast is the B<sub>2</sub> and DO<sub>3</sub> ordered phases of high silicon steel. When true strain is 0.3, white contrast area is larger, and then obviously reduced, meanwhile, arranged as small dispersed blocks in  $\varepsilon = 0.6$ . The degree of order decreases gradually with deformation, the strain softening behaviour occurs.

## 4. Conclusions

The softening behaviour of Fe-6.5%Si steel during warm deformation at 600 °C was investigated. The variety of work hardening exponent, Vickers hardness, indentation surface morphology and ordered degree during warm forming process is analysed.

- (1) The work-hardening exponents in different strain are calculated by the true stress–strain curve at 600 °C, the work-hardening exponent is on the rise when true strain is less than 0.2, and tends to decrease with respect to the true strain above 0.2.
- (2) When the strain is less than or equal to 0.3, hardness of the sample improves with the increase of deformation. When the strain is greater than 0.3, the hardness value of the sample has a slightly downward trend, with the increase of deformation. After the warm deformation at 600 °C, the work hardening exponent of the experimental steel has a drop.
- (3) The diffraction patterns intensity and dark field morphology of ordered phases indicate that the experiment steel is gradually less ordered with the raised deformation during warm deformation at 600 °C, this disordering contributes to strain softening behaviour of Fe-6.5%Si steel.

The financial support of National Natural Science Foundation of China (51174057, 51274062), the National High Technology Research and Development Program (2012AA03A503) and Research Fund for the Doctoral Program of Higher Education of China (20130042110040) are greatly acknowledged.

## References

- [1] T.P. Phway, A.J. Moses, *J. Magn. Magn. Mater.* **320**, 611 (2008)
- [2] W.J. Yuan, J.G. Li, Q. Shen, L. Zhang, *J. Magn. Magn. Mater.* **320**, 76 (2008)
- [3] T. Ros-Yanez, D. Ruiz, J. Barros, Y. Houbaert, *J. Alloys Compd.* **369**, 125 (2004)
- [4] M. Komatsubara, K. Sadahiro, O. Kondo, T. Takamiya, A. Honda, *J. Magn. Magn. Mater.* **242–245**, 212 (2002)
- [5] H. Fu, Z. Zhang, Q. Yang, J. Xie, *Mater. Sci. Eng. A* **528**, 1391 (2011)
- [6] J. Alcala, A. C. Barone, M. Anglada, *Acta Mater.* **48**, 3451 (2000)
- [7] S.H. Jiang, W.M. Mao, P. Yang, F. Ye, *Journal of University of Science and Technology Beijing* **36**(12), 1643 (2014) (in Chinese)
- [8] J.S. Shin, J.S. Bae, H.J. Kim, *Mater. Sci. Eng. A* **407**, 282 (2005)